CHALMERS

Evaluation of a non-isolated charger

Concept, analysis and reference design

Master of Science Thesis

ROBERT NYSTRÖM
YUXUAN HE

Department of Energy and Environment
Division of Electric Power Engineering
CHALMERS UNIVERSITY OF TECHNOLOGY
Göteborg, Sweden 2012

Evaluation of a non-isolated charger

Concept, analysis and reference design

ROBERT NYSTRÖM
YUXUAN HE

Department of Energy and Environment
Division of Electric Power Engineering
CHALMERS UNIVERSITY OF TECHNOLOGY
Göteborg, Sweden 2012

Evaluation of a non-isolated charger
Concept, analysis and reference design
ROBERT NYSTRÖM
YUXUAN HE

Department of Energy and Environment
Division of Electric Power Engineering
Chalmers University of Technology
SE–412 96 Göteborg
Sweden
Telephone +46 (0)31–772 1000

Cover:
Picture of an inductor, taken at Chalmers University of Technology.

Chalmers Bibliotek, Reproservice
Göteborg, Sweden 2012

Evaluation of a non-isolated charger
Concept, analysis and reference design

ROBERT NYSTRÖM
YUXUAN HE
Department of Energy and Environment
Division of Electric Power Engineering
Chalmers University of Technology

Abstract

This report discusses the necessity of a galvanic isolation in an onboard charger for a Plug-in Hybrid Electric Vehicle. It was hypothesized that the galvanic isolation was a source of losses, and it is known that the use of galvanic isolation give rise to higher costs and it requires more space. Three different topologies without galvanic isolation was investigated and simulated in OrCad PSpice. For these, cost, volume, weight and efficiency was analyzed and a best solution was chosen.

It was found that using a bridgeless charger gave the highest efficiency, approximately 98%, and it also had acceptable price and a satisfactory dimensional analysis. The bridgeless charger did however not perform good regarding THD injected into the utility, thus future work with this charger is needed to investigate if it is possible to reduce the THD impact without influencing the efficiency, size and weight to much. Synchronous rectification was also investigated and it was found that it was not a good solution in this case.

Index Terms: non-isolated, Power factor correction, onboard charger, bridgeless, fullbridge.

Acknowledgements

This work has been carried out at the both the Department of Energy and Environment at Chalmers University of Technology and at Volvo Cars. The financial support given by both in terms of computers, laboratories and supervision. A big thanks to Anders Magnusson and Mats Nilsson at Volvo Cars for supervision and for help regarding power electronic design. Thanks to Department of Energy and Environment and especially Torbjörn Thiringer for being our examiner.

Robert Nyström & Yuxuan He
Göteborg, Sweden, 2012

Contents

Chapter 1

Introduction

The increased popularity of Plug-in Hybrid Electric Vehicles (PHEV) increase the demands on the manufacturers to provide an energy efficient solution. The by far most available grid connection in Sweden is AC which makes it important to use an AC/DC conversion. In standard converters, the power factor can be as low as 50% resulting in low efficiency and high amount of harmonics due to the drawn current waveform [7]. To maximize the power output and minimizing the Electromagnetic Interference (EMI), the use of power factor correction can be used to emulate a resistive load. This method gives rise to a number of different topologies. These naturally consist of different components and control strategies which results in different cost and efficiency.

1.1 Problem background

Today, there is a preference of using galvanic isolation when it comes to on-board chargers. This isolation can of course cause higher weight, volume, price and might influence the efficiency of the converter. The high voltage system in the car is already galvanically isolated, thus there is actually no compelling need for isolation in the charger. In this project a galvanically isolated reference charger developed by Eltek is used. This chargers main attributes are considered as the goal of the new topologies evaluated.

1.2 Purpose

The purpose of this project is to investigate the efficiency for three chargers with different topologies, all without galvanic isolation, and to compare it with a reference design. Apart from testing efficiency, a cost estimation as well as power factor and Electromagnetic Interference (EMI) are targets to be investigated. The use of synchronous rectification is also to be investigated in order to determine if the efficiency can be increased. Finally the safety aspect will also be discussed, does the removal of isolation influence the safety of the charger?

1.3 Method and Scope

Method

To find alternative topologies and methods to implement a Power Factor Correcting (PFC) charger, IEEE Xplore and course material were used. To evaluate the alternative topologies the circuits were built in Cadence OrCad and simulated with PSpice. From PSpice, data was exported to Mathworks Matlab where efficiency, power factor and the Total Harmonic Distortion (THD) among other things were calculated and plotted. For the cost analysis, prices were taken from home pages or by contact with known suppliers. The price estimations were done for $>$10000 units, as this would be the case if the proposed charger were to be used and produced by Volvo. All results such as efficiency, power factor, THD, price, weight and volume will be compared with a known reference design.

Scope

The efficiency of the reference charger is 94% at full load and thus no topologies with a lower measured or estimated efficiency will be covered in this report. The price is also of concern which excludes all topologies considered too expensive. Apart from experiments performed on the reference charger, this project will only use simulations for the evaluation. No circuits will be constructed and tested. The project is also limited to 20 weeks.

Chapter 2

Theory

This chapter aims to give the required knowledge to fully comprehend the scope of the project.

2.1 Topologies

In this project three topologies were chosen, simulated and compared, and they are conventional-, bridgeless- and fullbridge converter. Generally, these topologies function as AC/DC converters, providing the AC side with high power factor and assuring a constant DC output.

2.1.1 Conventional

The conventional converter consists of three stages as shown in figure 2.1. The first stage is a diode bridge which rectifies the AC voltage to DC. The second stage is a boost converter which uses (PFC). The theory of PFC will be further explained in Section 2.2. The last stage is a DC/DC stage which makes the output voltage more stable and also increase the range of the output voltage.

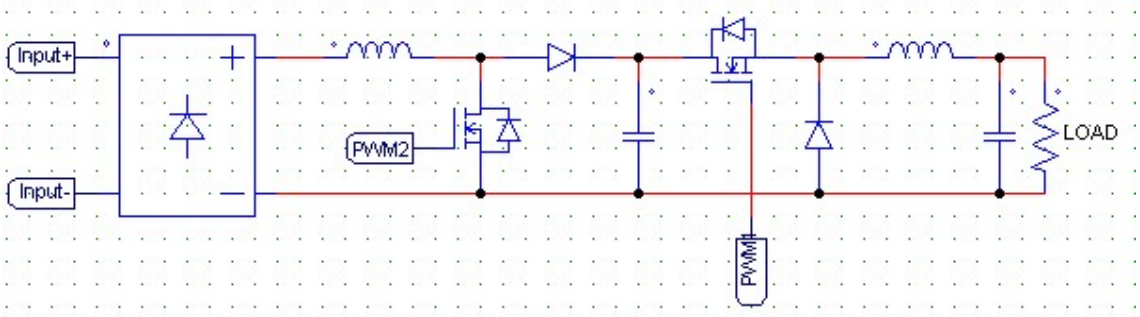

Figure 2.1: Conventional Converter

2.1.2 Bridgeless

Figure 2.2 shows the bridgeless converter, which works in a quite similar way to the conventional. In fact it is two conventional converters taking care of one half of the period each. In this way there is no need for a rectifier stage. It consists of two stages, one boost converter and one DC/DC stage to stabilize the output and increase the voltage range.

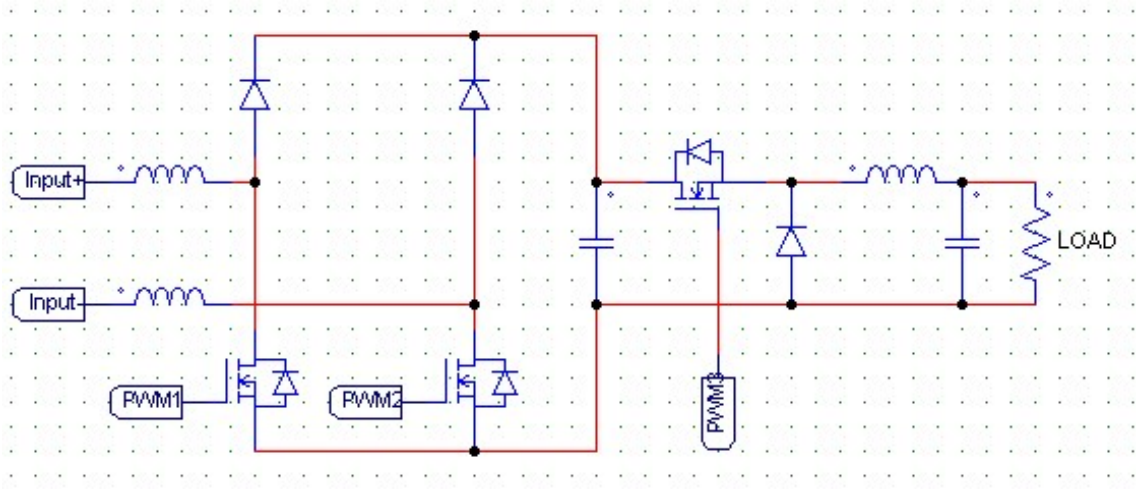

Figure 2.2: Bridgeless Converter

2.1.3 Fullbridge

The topology of the fullbridge converter is presented in figure 2.3. One advantage of this topology is that it only requires one stage to achieve a constant DC output without low frequency ripple. Furthermore, since there is no diode in the circuit, the full bridge converter doesn't give any crossover distortion in the input current, and the THD is reduced. Crossover distortion will be further discussed in Section 4.1.

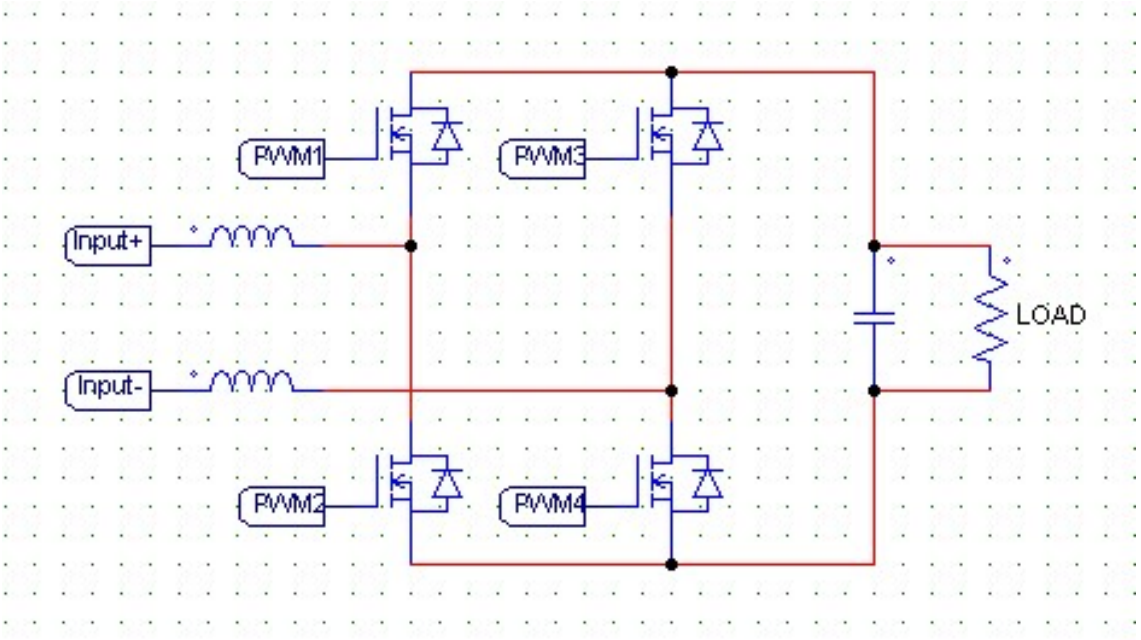

Figure 2.3: Fullbridge Converter

The disadvantage is that it requires two high-side drivers which increase the complexity and cost of the MOSFET driving system. Another drawback is that the output capacitance is higher compared with the bridgeless PFC converter, which makes the capacitor bigger and it might not fit in the enclosure.

2.2 Power Factor Correction

When constructing a commercially available charger one of the most important aspects is the power factor (P.F.). The power factor is defined as $P.F. = \frac{P}{S}$ where P is real power and S is apparent power [3]. Only real power can be used by the load, and thus we want the apparent power S to appear as equal to P as possible. This would give a power factor $P.F. = 1$ or $P.F. = 100\%$. The power factor consists of two parts as

$$P.F. = \underbrace{\cos(\Phi)}_{Displacement factor} \quad \underbrace{\sqrt{\frac{1}{1 + (I_2/I_1)^2 + (I_3/I_1)^2 + \cdots}}}_{Distortion factor} = \frac{\cos(\Phi)}{\sqrt{1 + (THD)^2}} \tag{2.1}$$

where the displacement is tied to the phase shift between the voltage and current, and distortion is tied to the *Total Harmonic Distortion* (THD). The THD describe how much of the total transmitted power, the apparent power *S*, that consists of harmonics [3]. The distortion component i_{dis} is written as

$$i_{dis}(t) = i_s(t) - i_{s1}(t) = \sum_{h \neq 1}^{\infty} i_{sh}(t) \tag{2.2}$$

where h declares the order of the harmonic, i_s is the total current and i_{s1} is the current in the fundamental frequency. The THD is then defined as

$$\%THD = 100 \cdot \frac{i_{dis}}{i_{s1}} = 100 \cdot \sum_{h \neq 1}^{\infty} \frac{i_{sh}}{i_{s1}} \tag{2.3}$$

and is thus a quota between the sum of all harmonics and the current in the fundamental frequency. Apart from influencing the efficiency there are regulations on the amount of *Electromagnetic Interference* (EMI) an electrical device is allowed to inject into the utility. As THD influence both the efficiency and is regulated it is vital to keep it low and to avoid creating current harmonics it is important that the current and voltage waveform have the same shape, i.e. the load emulates a resistance. A regular rectifier is not a linear load, as seen by the waveforms in figure 2.4, and thus injects harmonics into the utility grid.

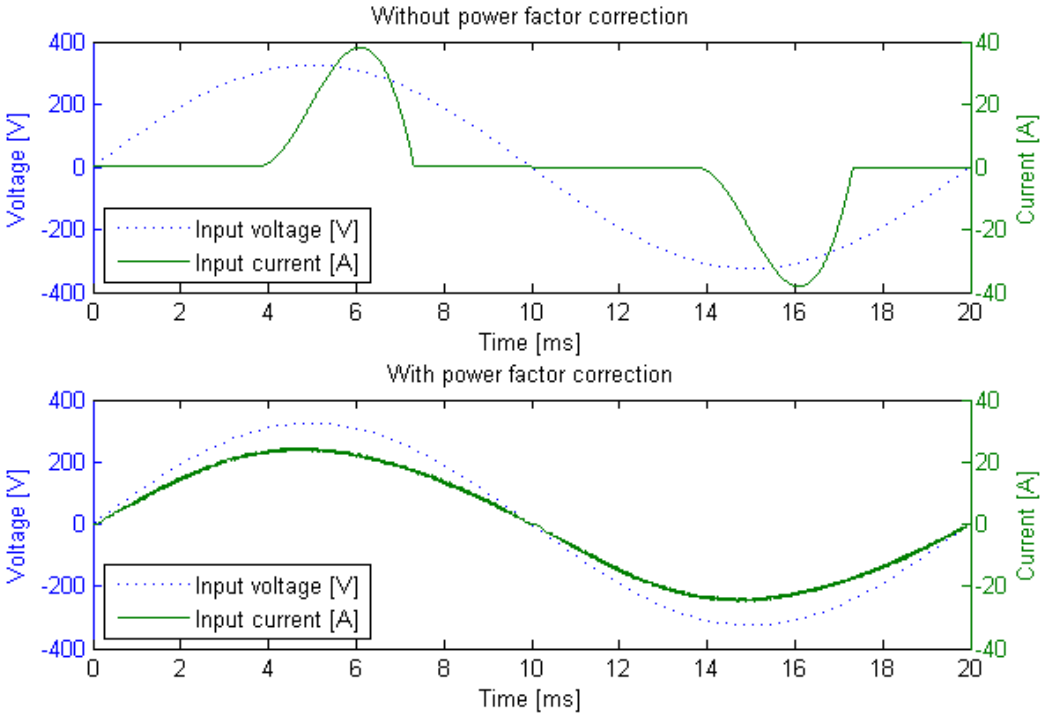

Figure 2.4: The difference between Power Factor Corrected and a regular rectified current versus voltage.

Without any kind of correction, a P.F. of $50\% - 70\%$ is common and in most cases this distortion is a pure loss [7]. With the use of passive filters the linearity can be improved and the P.F. higher but as some of the harmonics have a frequency of only $150\ Hz$, the capacitance and inductance in the filter needs to be large which drastically increase both cost and size of the components.

A better way to solve this problem is by using active *Power Factor Correction* (PFC) which controls the current flow with MOSFETs or IGBTs. The most common way to implement PFC is by using a boost converter and replace the control system with a PFC control system [7]. There is several ways to construct the control system, but in this project the current mode control was used and will be explained.

This control strategy uses two PI-regulators, one for the voltage and one for the current. See figure 2.5 for an overview of the control strategy.

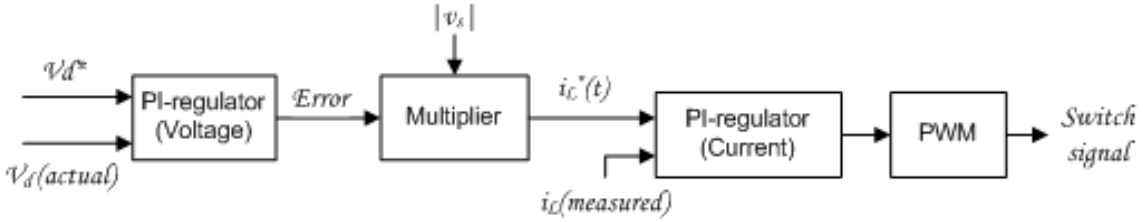

Figure 2.5: Overview of the control strategy.

The outer loop is the voltage loop and compares the measured output voltage with a reference value. The PI-regulator controls this error and will increase/decrease the amplitude of the control signal if the output is to low/high. This amplitude will then be

multiplied with an absolute valued measurement of the input voltage which will give the control signal the correct shape, namely a sinusoidal.

The inner loop contains a PI-regulator for the current control. It compares the sinusoidal reference from the outer loop with a measured current from the input side. From the current loop the control signal is input to a PWM circuit, which creates the switching pattern for the transistors.

It is thus the voltage loop that controls the output level and the current loop controls the shape. If the output voltage is to low the amplitude of the current reference will be larger and thus inject more power into the charger and vice versa if the voltage is to low. How the control loops are implemented will be further described in Section 3.2.6

2.3 Design of inductor

The design of an inductor is very significant in this project, because it largely impacts the performance and losses of the system. The design of a inductor has some constraints: First, the core of the inductor should work within the saturated flux density with the given maximum current. Secondly, the window area should be large enough for the wire to fit through. Finally, the number of turns is preferred to be small to give shorter wire length for the conductor and thus a smaller winding resistance.

Considering the above constraints the inductor was designed according to the following steps:

1. Find I_{max}, the maximum current through the windings.
2. Search in a core database to find one or a number of cores with saturation current greater than I_{max}.
3. Calculated the number of turns according to

$$n = \sqrt{\frac{L}{AL}} \tag{2.4}$$

where the AL-value is given by the manufacturer and have the unit $[\frac{H}{n^2}]$.

4. Select the copper area A_w which gives the maximum current density less than $4A/mm^2$
5. Calculate the necessary window area as $n \cdot A_w$ and find the best core where the wire will fit.
6. Calculate MLT (Mean length per turn) and the winding resistance by

$$R = \rho \frac{(MLT) \cdot n}{A_w} \tag{2.5}$$

where ρ is the resistivity of copper, $\rho = 1.75e^{-8}\,\Omega/m$.

2.4 Loss calculations

The loss over each component is interesting to estimated since it influences the efficiency of the system and it's a necessary data for the thermal analysis and heat sink design. All

the losses discussed in this thesis are average power losses during one cycle of $20\ ms$, since the losses during one switching period vary greatly. The energy can be calculated by

$$E_{Loss} = \int_0^T P(t)dt = \int_0^T V(t)I(t)dt \tag{2.6}$$

where E_{Loss} is the energy consumed during one cycle, T is the time of one cycle, V(t) and I(t) are the voltage and current over the component respectively. Then the power loss is calculated as

$$P_{Loss} = \frac{E_{Loss}}{T} \tag{2.7}$$

2.4.1 Thermal calculations

Thermal analysis is an important part of the design since a proper cooling method should be used to control the temperature and avoid damage to the electric components. The temperature of the junction of electric components can be calculated as

$$T_j = (R_{jc} + R_{cs} + R_{sa})P_D + T_a \tag{2.8}$$

where T_j is the junction temperature, R_{jc} is the junction to case thermal resistance, R_{cs} is the case to heat sink thermal resistance, R_{sa} is heat sink to ambient thermal resistance, P_D is the power dissipation and T_a is the ambient temperature.

Chapter 3

Case set-up & Design

This chapter will describe the set up of the project, what was given and what was required as a result. It will also show the components and the PSpice schematics used to evaluate a charger topology as well as describe how the different charger topologies work and behave.

3.1 Requirements

As this project was set up to find a improved design of a on board charger there is a number of specifications from a reference design that needs to be considered. In Table 3.1 the specification of the reference charger is shown, and as the goal is an improved design the new topologies should match or be better than these.

Table 3.1: The specification of the reference charger this project aims to supersede.

Units	Requirement
Input voltage	$85 - 275\ V_{ac}$
Input current	$14\ A_{rms}$
THD	$< 5\%$
PF at 50% load	$> 99\%$
Efficiency at full load	$> 94\%$
Output voltage	$250 - 450\ V_{dc}$

3.2 Conventional charger

The conventional charger is the method usually implemented for PFC [8]. This charger was the first one constructed within this project and can be seen in figure 3.1. Hierarchial blocks was used to simplify the circuit and make it easier to overlook. This made both design and troubleshooting easier.

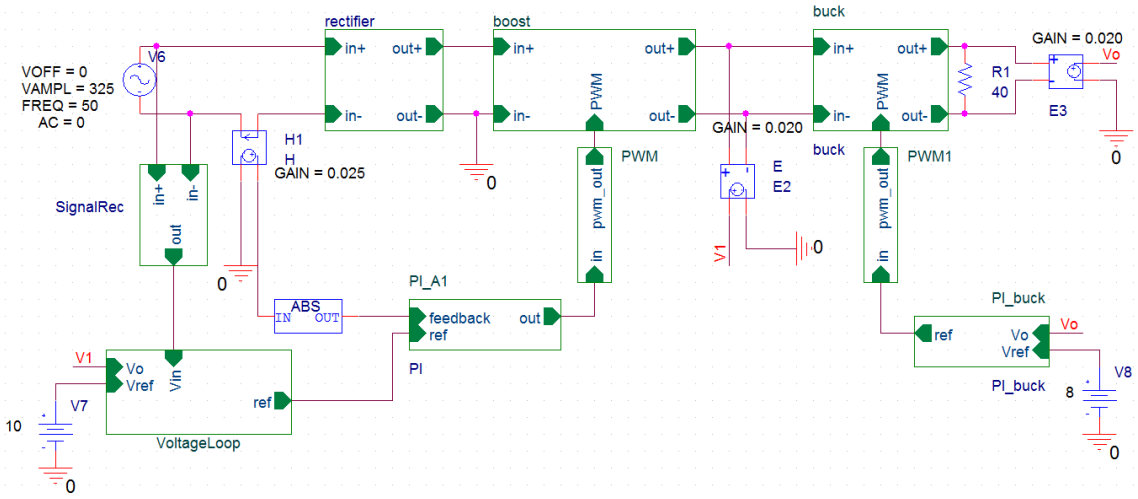

Figure 3.1: The Conventional Charger.

To decrease the time required for simulation initial values were set for the capacitors and in some cases the control system. By adding *ic*=-<*VALUE*> after the impedance property in PSpice an initial condition is set, i.e. $500u\ ic = -400$ to have a capacitor of $500\ \mu F$ with a initial voltage of $400\ V$.

3.2.1 Input and output

As input into the charger a *VSIN* voltage source was used. The parameters where chosen to create similar conditions as if the real charger would be connected to the utility grid in Sweden. The amplitude of $325\ V$ represents the effective value of $230\ V$. There were also tests performed corresponding an amplitude of $85 \cdot \sqrt{2} = 120\ V$ to see how the chargers behaved in a worst case scenario for grids with a lower voltage of $110\ V_{rms}$.

3.2.2 Rectifier

Noticeable with the conventional topology is the use of three stages, rectifier, boost and buck converter. The rectifier is the first stage and was implemented as a full wave rectifier according to figure 3.2.

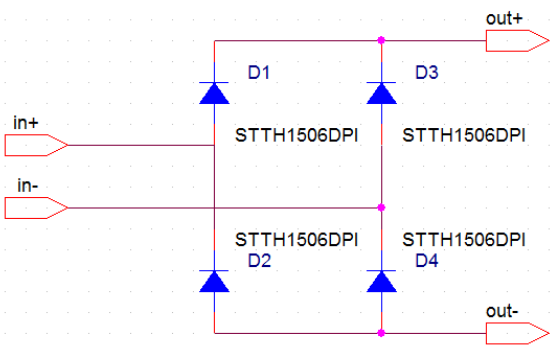

Figure 3.2: The full wave rectifier used for the conventional charger.

This stage is necessary as the conventional converter can't rectify by it self.

3.2.3 Converter

The second stage is the boost converter and together with active control to shape the input current. The output was somewhat DC but with quite high oscillations. The boost stage can be seen in figure 3.3.

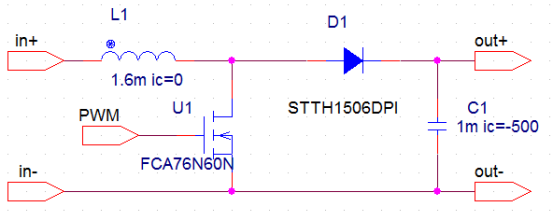

Figure 3.3: The boost converter used in the conventional charger.

3.2.4 Buck converter

To increase the voltage range to what the reference design had, see Table 3.1, a buck converter was necessary, see figure 3.4. Apart from making the output voltage range larger the buck converter had a output with a very low amount of ripple.

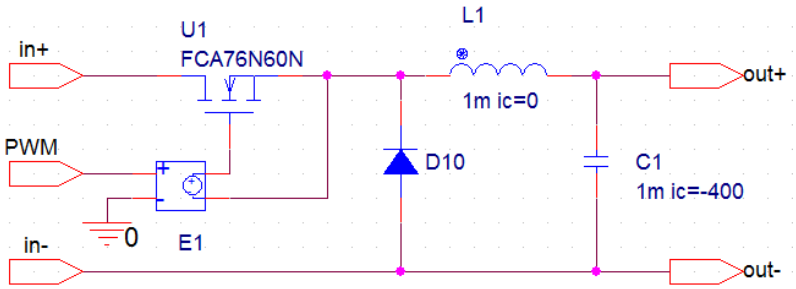

Figure 3.4: The buck converter used in most chargers.

This third stage does have its drawbacks, however. The result is higher total power loss and potentially higher price for constructing the charger. The control for the buck converter was not integrated with the other parts of the control system. It is a regular PI-controller with a PWM module to control its MOSFET, see figure 3.5. The PWM module will be further explained in Section 3.2.7.

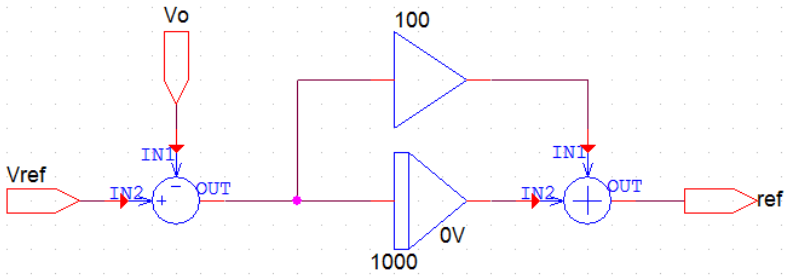

Figure 3.5: The PI-controller for the buck converter.

The controller was needed to be fast both to allow fast response and to dampen possible oscillations created by the previous stage. The values are $k_p = 100$ for the proportional gain and $k_i = 1000$ for integral gain.

3.2.5 Signal rectifier

To create a suitable reference for the control system the input voltage had to be rectified. This block, seen in figure 3.6, do this by measuring the potential difference over the input voltage source. The difference is then scaled down to a suitable level that the control system can handle and rectified with a mathematical block called *ABS*.

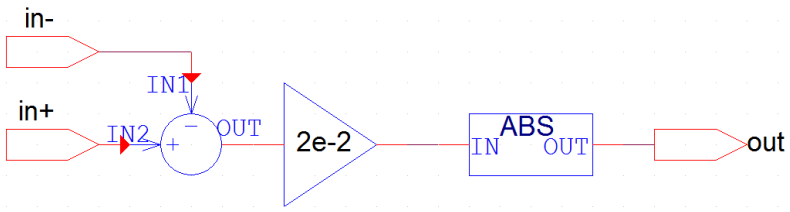

Figure 3.6: The signal rectifier was used to measure the absolute value of the voltage.

3.2.6 Control loops

To control the output voltage, current-mode control were used, see figure 3.7 for the construction of the voltage controller.

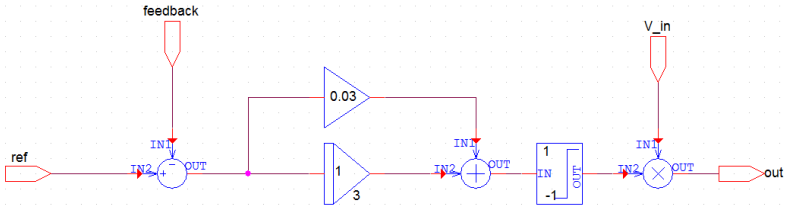

Figure 3.7: The voltage controller used in most circuits.

As the output voltage in most cases where oscillating it was found that this controller worked best with a very slow controller to dampen the oscillations in the current reference. The current reference will appear to become ”out of phase” as the output from the PI-controller is multiplied with the measured input voltage which also is sinusoidal. The drawback with using a slow PI-controller for the voltage is that it takes longer time for the converter to reach steady state. However, in all cases the converters reached steady state within $500\,ms$ which was considered to be within the limits. In figure 3.8 the current controller is shown. The construction is identical but the PI-parameters are different.

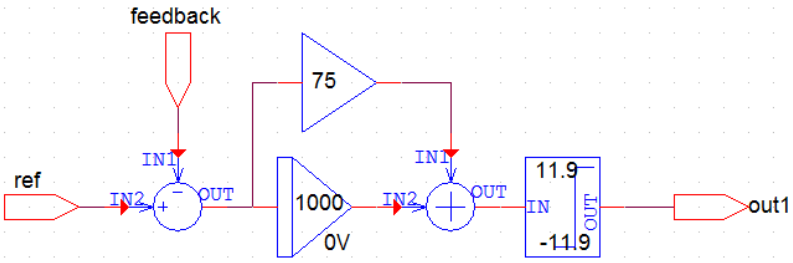

Figure 3.8: The current controller used in all circuits.

The implementation was done in steps and first the current loop was implemented and tuned with a current reference from an ideal VSIN voltage source. With a constant

sinusoidal current reference the output voltage was not good but neither of importance, the focus was at finding a controller which followed the sinusoidal reference. The resulting PI-parameters were 75 for the proportional gain and 1000 for the integral gain. The reason for a big proportional gain is the need for a very fast response. A slower response with only high integral gain results in a noticeable crossover distortion, more information and figures in Section 4.1.

When the current controller works good, the voltage controller is given the task to deliver the current reference. In this stage the whole control circuit was implemented and tested, trying to find the most optimal PI-parameters for the voltage controller. The resulting values is 0.03 for the proportional gain and 1 for the integral gain. Compared to the current controller the voltage controller is much slower.

3.2.7 PWM

Pulse Width Modulation (PWM) were used to control the MOSFETs. The principle of the PWM is a comparison between a triangle wave and a certain voltage level which will create a Pulse with a certain duty cycle i.e. the time the output signal is 1 or 0. A duty cycle of 0.5 or 50% means the pulsing output is 1 respective 0 half of the time. The frequency of the triangle wave determines the output frequency. A triangle wave with a frequency of $45KHz$ with a voltage range between $-12V$ to $12V$ were used. In PSpice the comparator was a programmed ideal function block, see figure 3.9.

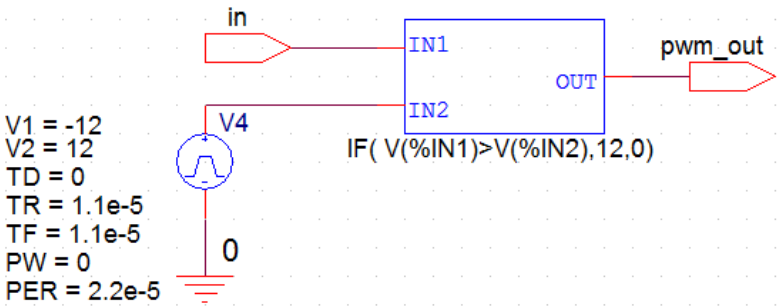

Figure 3.9: The PWM module used is a programmed ideal function which compares the different inputs.

The triangle wave was created by a regular *VPULSE*, usually used to create square waves. The properties for the *VPULSE* can be seen in figure 3.9. The first two properties, *V1* and *V2*, is the voltage range, *TD* is the delay, *TR* and *TF* is the rise and fall time respectively, *PW* is the pulse width and *PER* is the period. By setting the sum of the rise and fall time equal to the period and the pulse width to 0, a triangular wave is created. Although some chargers had different solutions to the PWM-module, the principle was always the same.

3.2.8 MOSFET Driver

A MOSFET driver is needed to amplify current to increase the commutation speed and apply control voltage over source and gate of the MOSFET in high-side case. In practice, MOSFET driver ICs, for instance *IR2110* from *International Rectifier* or other BJT drive

circuits are used. However, to simplify the simulation and reduce the simulation time, an ideal voltage controlled voltage source is implemented as the MOSFET driver. This method is used in the buck converter and is shown as *E1* in figure 3.4.

3.2.9 Chargers load

As load to emulate a battery a regular resistance was used. To find the optimal design under different operation points the charger were simulated with a load resistance that was swept across a range between $34\ \Omega$ and $194\ \Omega$. This is done with a block called *PARAM* and the use of global variables in Cadence OrCad. With this range of resistance the power level could be varied between $1300\ W$ and $3600\ W$.

3.3 Bridgeless charger

The bridgeless charger was the second charger constructed and as can be seen in figure 3.10 only use two stages, a boost converter and a buck converter. It is actually possible to use only the boost converter, but to fulfill the projects requirements regarding output ripple and voltage range another stage was necessary.

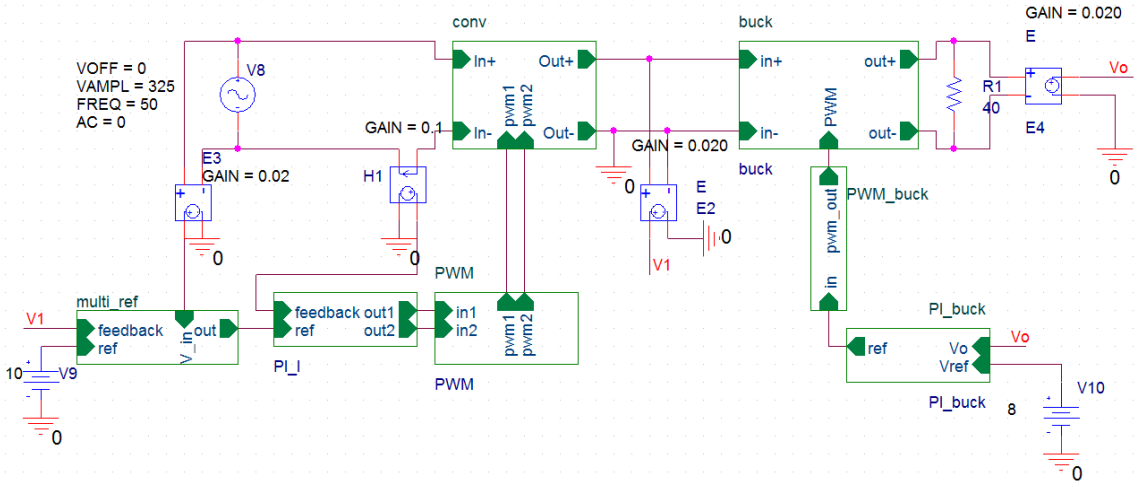

Figure 3.10: The Bridgeless Charger.

This converter used the same method for the buck converter, control system and PWM module as the conventional topology. These are described in 3.2.4, 3.2.6 and 3.2.7 respectively. The boost converter is however unique.

3.3.1 Converter

The bridgeless converter implemented in OrCad can be seen in figure 3.11.

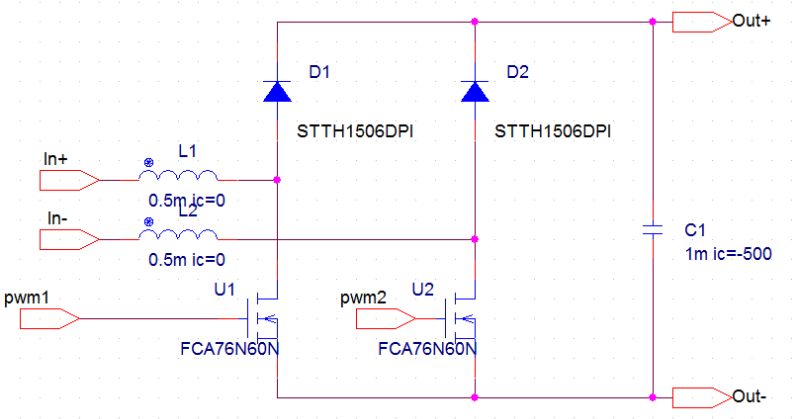

Figure 3.11: The boost stage of the bridgeless charger.

3.4 Fullbridge charger

The fullbridge charger evaluated can be seen in figure 3.12. As seen in the figure the fullbridge only consists of one stage.

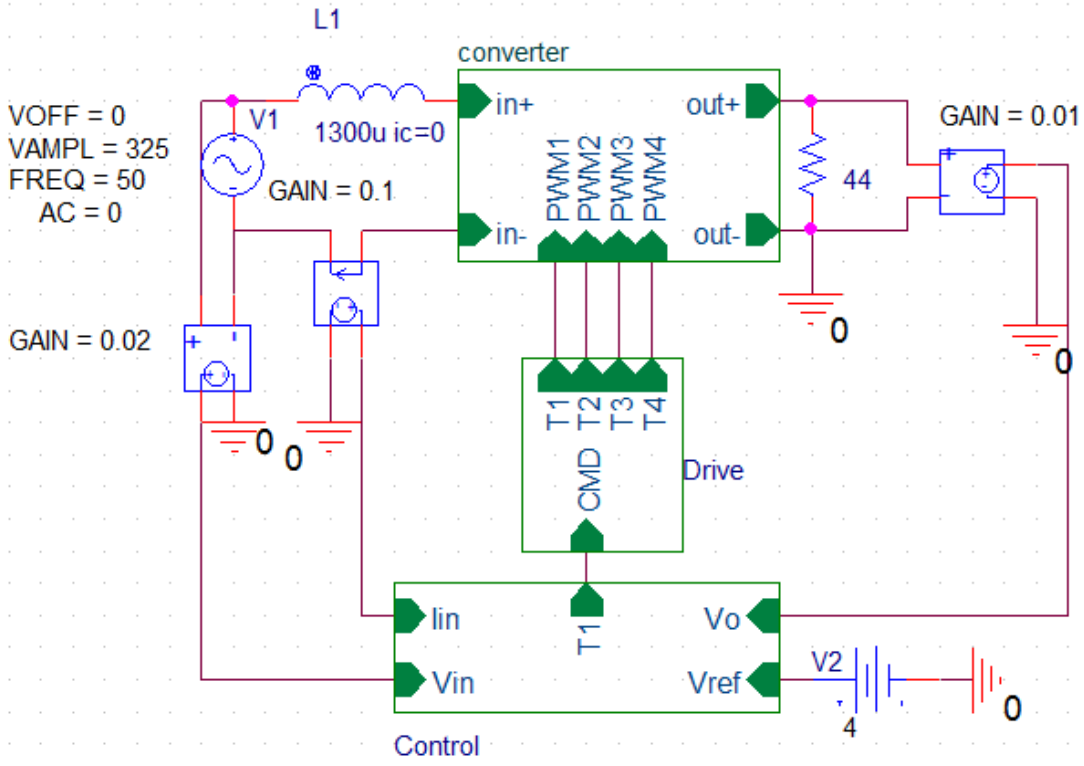

Figure 3.12: The fullbridge charger.

3.4.1 Converter

The topology of the full bridge converter is shown in figure 3.13. In the simulation, in order to simplify the design, the voltage controlled voltage sources are used as both high side and low side driver.

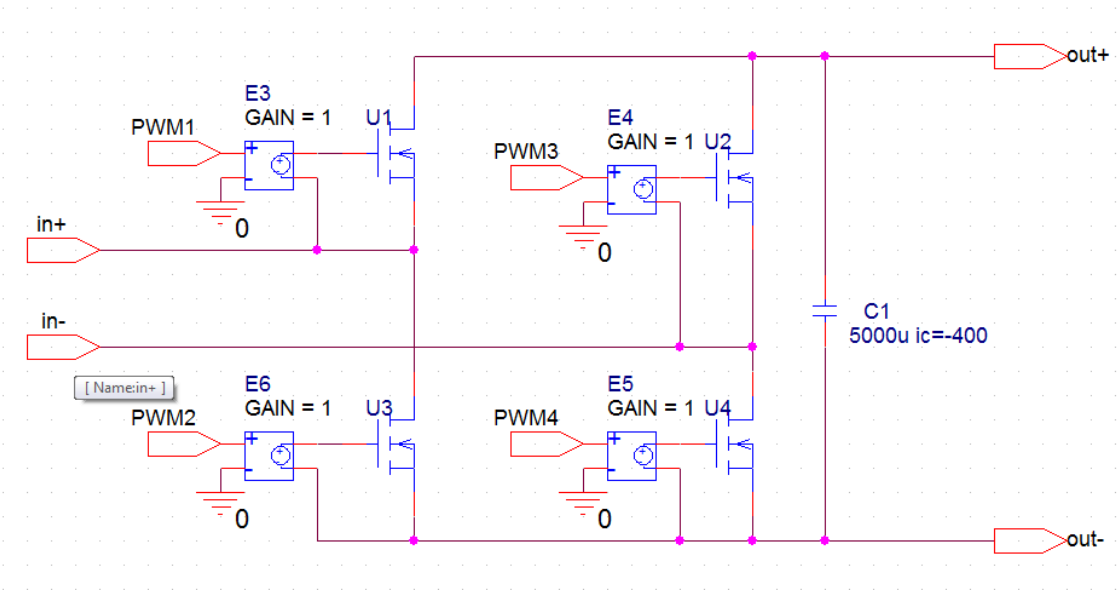

Figure 3.13: The fullbridge converter.

The control system is the same as for the other chargers and is described in 3.2.6.

3.4.2 PWM control

The control of the full bridge converter is presented in figure 3.14. In this design, *Bipolar Voltage Switching* is used. MOSFET 1 and MOSFET 4 use the same PWM signal which is opposite to the signal of MOSFET 2 and MOSFET 3, all visible as U1 to U4 in figure 3.13. It should be pointed out that in practice a blanking time is needed to ensure one switch is completely turned off before turning on the other switch in the same leg. This blanking time will introduce distortion in the input current [3].

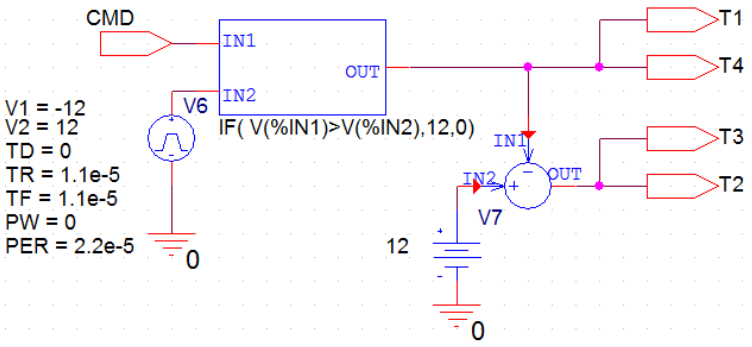

Figure 3.14: The PWM control of the fullbridge.

3.5 Components

In the three constructed chargers the same components were used and these will be described in this section. There will be an explanation on why the specific component was chosen as well as special requirements that was needed to be considered.

3.5.1 Diodes

The diode used with all chargers had a couple of requirements it had to fulfill. It had to be able to block a voltage of $600\ V$, handle a current of $20\ I_{rms}$, have a low forward voltage drop and be fast to decrease the losses. All these requirements have a margin to decrease the amount of components destroyed. The diode found is a *STTH1506DPI* from *ST Microelectronics*. It's main characteristics can be seen in Table 3.2.

Table 3.2: The main characteristics of the chosen diode, STTH1506DPI [4].

Symbol	Parameter	Value	Unit
V_{RRM}	Repetitive peak reverse voltage	600	V
$I_{F(rms)}$	RMS forward current	26	A
V_F	Forward voltage drop	3.6	V
t_{rr}	Reverse recovery time	16*	ns

*typical value

This diode consists of two $300\ V$ diodes connected in series. That is why the forward voltage drop is quite high compared to regular diodes. It is however very fast, which will make the switching and also the total losses low.

3.5.2 MOSFET

Since a quite high switching frequency is required by this design and lower losses are preferred, a MOSFET was selected to work as a switch. Compared with an IGBT, a MOSFET doesn't have the forward voltage drop, thus the losses will be lower. A MOSFET can also switch up to $100\ kHz$ or higher, which makes it the ideal choice in this case as the frequency is more likely to increase than decrease during improvement of the charger [3]. The requirements for selecting the MOSFET are as follows. First, the voltage and current over the MOSFET are approximately $300\,V$ and $20\,A$ respectively. Considering the safety criteria, the MOSFET should handle a voltage of $450\ V$ and a current of $30\ A$ at least. Secondly, the series resistance R_{DS} should be as small as possible to achieve lower conducting losses. Finally, the turn on and turn off time need to be short to reduce the switching losses. According to these requirements, MOSFET *FCA76N60N* from *Fairchild* was selected. The key parameters can be found in Table 3.3.

Table 3.3: The main characteristics of the chosen MOSFET, FCA76N60N [2].

Symbol	Parameter	Value	Unit
V_{DSS}	Drain to Source Voltage	600	V
I_D	Drain Current	76	A
R_{DS}	Static Drain to Source On Resistance	28	$m\Omega$

Worth noting is the high I_D. A MOSFET designed for higher currents have a smaller R_{DS} without a large increase in price. Thus is the component over dimensioned in order to decrease the losses.

3.5.3 Inductor

In this project, two inductors had to be designed: the inductor at PFC stage and at the output filter. The inductance value at PFC stage determines the input current ripple and further influences the THD and the harmonics. To calculate the inductor, the tolerated current ripple is defined to be 10% so the maximum current ripple can be expressed as

$$\Delta I_L = 10\% \cdot I_{in(pk)max} = 0.1 \cdot 16\sqrt{2} \approx 2.63\ A \tag{3.1}$$

where ΔI_L is the ripple current in the inductor, $I_{in(pk)max}$ is the maximum peak value of the current. To find an inductor that will suffice even for the worst case scenario, a voltage of $85\ V$ is considered. The peak value is found as

$$V_{in(pk)min} = V_{in(rms)min}\sqrt{2} = 85\sqrt{2} \approx 120\ V \tag{3.2}$$

The boost output voltage is set to $500\ V$ to have some margin for the second stage (buck converter) which will transform the output voltage over the load between $250 - 450\ V$. The peak boost transistor duty cycle is then calculated as

$$D_{pk} = 1 - \frac{V_{in(pk)}}{V_m} = 1 - \frac{120}{500} = 0.76 \tag{3.3}$$

The reference charger had a switching frequency of $45\ kHz$ and the same frequency was used in this case. Together with the values calculated in (3.1) - (3.3) the inductance is calculated as

$$L = \frac{V_{in(pk)min} \cdot D_{pk}}{f_{sw} \cdot \Delta I_L} = \frac{120 \cdot 0.76}{45e3 \cdot 2.63} = 771\ \mu H \tag{3.4}$$

This value gave a good estimation on a value to start with in the simulation. During the development of the circuits the values for the different chargers changed according to Table 3.4.

Table 3.4: Design of input inductor

Converter	Value	Unit	Quantity
Conventional	1600	μH	1
Bridgeless	500	μH	2
Fullbridge	500	μH	2

For both the bridgeless and the conventional converter, there was a need for an output inductor in the final stage. The output inductor impacts the output current ripple. Assuming the output capacitor is ideal, the duty cycle for a buck converter is

$$D = \frac{V_o}{V_m} = \frac{400}{500} = 0.8 \tag{3.5}$$

where V_o is the output voltage and V_m the input voltage. The ripple current for a buck converter is defined as

$$\Delta I_L = \frac{1}{L}\int_0^{DT_s} V_L dt = \frac{DT_s(V_m - V_o)}{L} = \frac{D(V_m - V_o)}{Lf_s} \tag{3.6}$$

The power is specified at $3600\,W$ during full load when the voltage is $400\,V$ which gives a current $I = \frac{3600}{400} = 9\,A$. The current ripple is required to be $\leq \pm 10\%$ which is $\pm 0.9\,A$ and thus gives a ripple current $\Delta I_L = 1.8\,A$. Rewriting (3.6) to solve for the inductance gives

$$L = \frac{D(V_m - V_o)}{\Delta I_L f_s} = \frac{0.8 \cdot (500 - 400)}{1.8 \cdot 45e3} = 987.65\,\mu H \tag{3.7}$$

This value was later found to be larger than necessary and it was finally set to $500\,\mu H$. [1]

The core found for the inductors is produced by Vacuumschmelze and is a toroidal core, the dimension are shown in Table 3.5.

Table 3.5: Size and weight of the inductor core [5].

T60006-L2063-W985

AL-value	Outer diameter	Inner diameter	Height	Weight
2.5 to 4.8 μH	63 mm	50 mm	25 mm	163 g

The outer radius and the height is made $5\,mm$ larger because of the windings. In the case of the height, there are windings on both sides while the radius is calculated from the middle and thus only consider the outer windings, see figure 3.15.

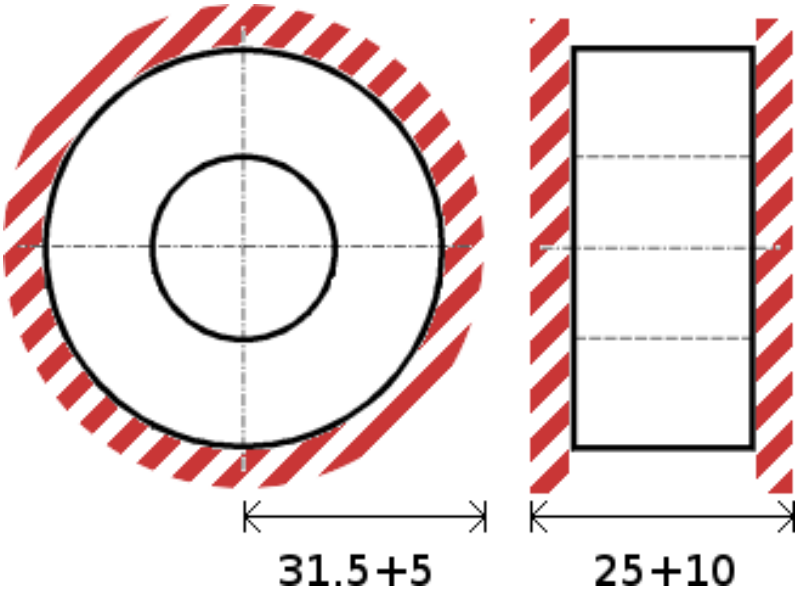

Figure 3.15: Inductor volume calculations including windings.

The volume for one inductor is thus approximately $(\frac{63}{2}+5)^2\pi \cdot (25+10) = 146.489e3mm^3$ or $0.1465\ dm^3$. The conventional charger only has one inductor so the total volume is $0.1465\,dm^3$ and a weight of $163\,g$ or $0.163\,kg$. Both the bridgeless and the fullbridge have two inductors, the total volume is $0.1465 \cdot 2 = 0.293\,dm^3$ and a weight of $163 \cdot 2 = 326\,g$ or $0.326\ kg$.

3.5.4 Capacitor

For the conventional and bridgeless converters, both the middle point and the output need a capacitor, and for the fullbridge, a capacitor only exists at output. The capacitor works

as the output filter, which determines the output voltage ripple and the hold up time. The maximum voltage ripple is required to be $< 10\,V$. The capacity can be found by

$$C \geq \frac{\frac{P_o}{V_o}}{2\pi f_r V} = 1.4\,mF \tag{3.8}$$

where f_r is the frequency that needs to be rectified, and in the worst case, $f_r = 100\,Hz$.

Considering the price and volume of the design, the capacitors were reduced to $940\,\mu F$ for the conventional and bridgeless converter. However, in order to fulfill the requirement, the capacitor was changed to $2720\ \mu F$ for the fullbridge converter. For the component selection part, capacitors with lower capacitance were connected in parallel to give the lowest price and lower internal resistor. The value and quantity of the capacitor is shown in Table 3.6.

Table 3.6: Design of output capacitor

Converter	Value	Unit	Quantity
Conventional	470	μF	2+2
Bridgeless	470	μF	2+2
Fullbrdge	680	μF	4

The capacitors chosen are *096 PLL-4TSI* produced by *Vishay*. In Table 3.7 the parameters important for calculations of the volume and weight are shown.

Table 3.7: Size and weight of the capacitors [6].

096 PLL-4TSI			
Capacitance	Diameter	Height	Weight
470 μF	35 mm	70 mm	103 g
680 μF	35 mm	80 mm	115 g

As the chargers had four capacitors the total volume for all chargers except the fullbridge is $4 \cdot (\frac{35}{2})^2\pi \cdot 80 \approx 269.39e3\ mm^3$ or equivalently $0.26939\ dm^3$ and a total weight of $103 \cdot 4 = 412\ g$ or $0.412\ kg$. In a similar manner the total volume for the capacitors in the fullbridge is found to be $0.30788\,dm^3$ and a total weight of $4 \cdot 115 = 460\,g$ or $0.46\,kg$.

Chapter 4

Analysis

This project has chosen to analyze three different topologies and compare it to a reference design, see figure 4.1.

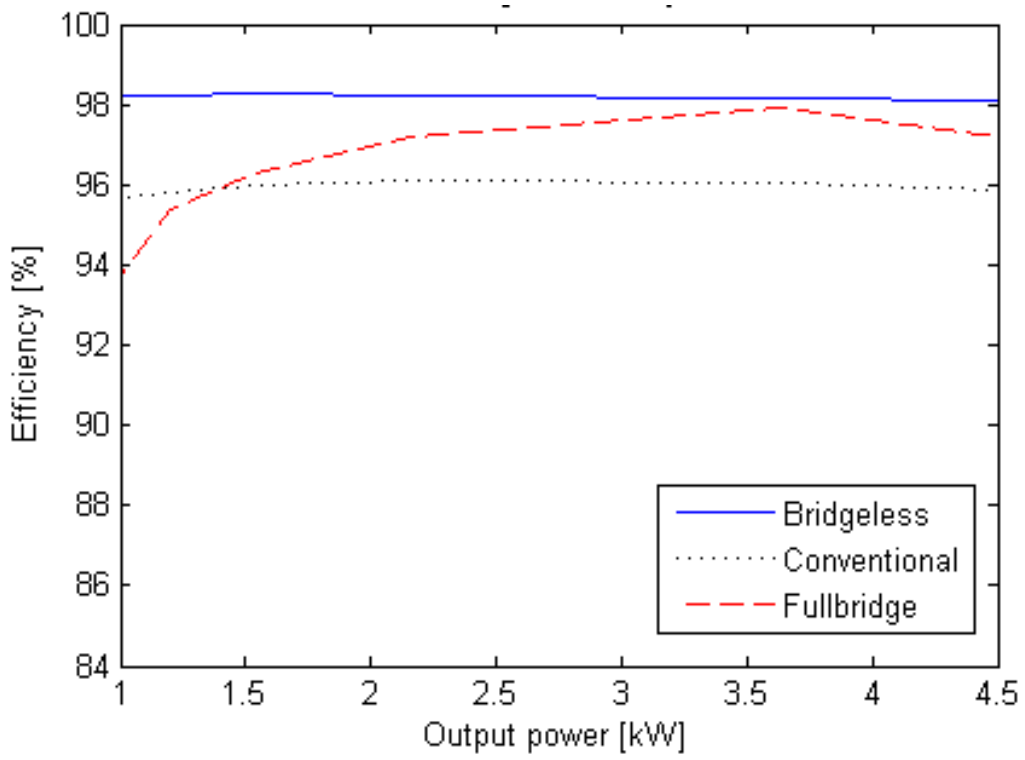

Figure 4.1: Charger efficiency with $230\ V$ input voltage

As can be seen in the figures above the fullbridge charger performed quite well. The conventional chargers performance is similar to the bridgeless, almost constant over the different power ratings but lower efficiency. These different properties makes it interesting to consider the performance during different power scenarios. Different charge cycles were not considered as it was assumed the chargers will use maximum power available for most of the time during charging. The reference charger is designed for a maximum of $230\ V$ and a $16\ A_{rms}$ which gives a power rating of $3.6\ kW$. In Sweden however, it is common to use a $10\ A$ fuse which limits the input power to $2.3\,kW$, thus all chargers have be evaluated for both these power ratings. The chargers will also most likely be used in other countries with a lower grid voltage and as a worst case scenario, an input voltage of $85\ V$ will be considered, for which the power output is $\approx 1300\ W$, see Table 4.1.

Table 4.1: The performance of the chargers during different input voltage and power limitations. For the P.F. all values are rounded from three decimals.

	Conventional			Bridgeless			Fullbridge		
Voltage	85 V	230 V^*	230 V	85 V	230 V^*	230 V	85 V	230 V^*	230 V
Efficiency	90.32%	96.13%	96.06%	98.98%	98.24%	98.17%	94.67%	97.23%	97.91%
P.F.	100%	99.91%	99.92%	100%	100%	100%	100%	99.92%	99.93%
THD	4.0%	8.32%	6.29%	6.32%	11.09%	7.20%	1.3%	4.68%	4.25%

* 10 A fuse, 2.3 kW limitation.

The losses for each component in the charger can be seen in more detail in Table C.1.

4.1 Harmonics & Waveforms

The frequency spectrums for the input current of the three topologies are shown in Figure 4.2. Since the harmonics at a higher frequency are almost invisible, only the first 32 orders harmonics are plotted. As can be seen, the third harmonics in the three converters are almost the same. The full bridge converter have the least amount harmonics at higher frequency, which verifies that full bridge converter has the lowest THD compared with others. However, it can also be noticed that the harmonics around 25th order increase again and this may be due to the design of the filter.

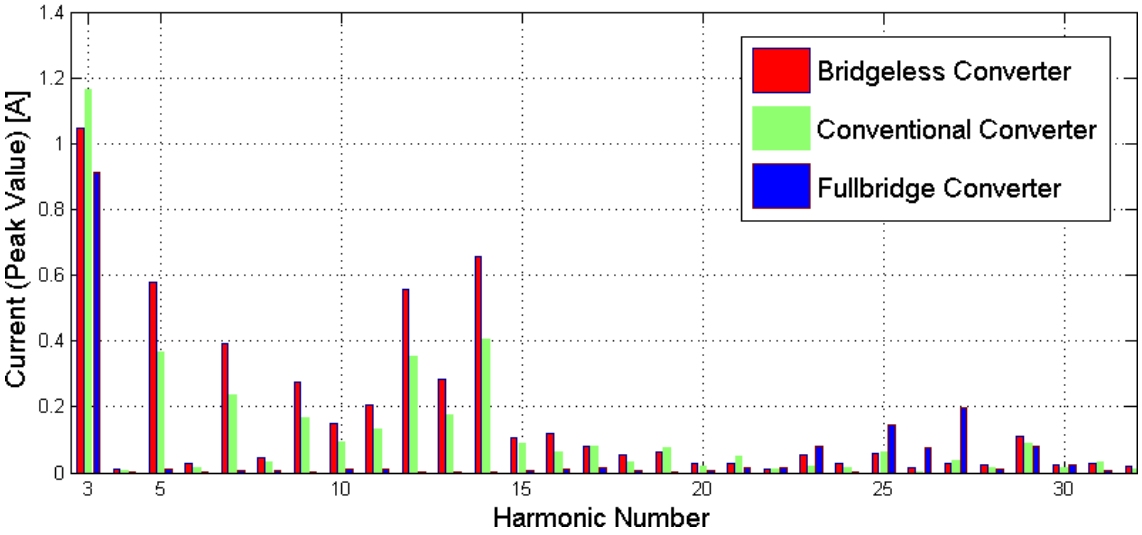

Figure 4.2: Frequency spectrums of different converters

Both the bridgeless and the conventional charger have quite high amount of harmonics up to the order of fourteen, most likely because of the crossover distortion, see figure 4.3.

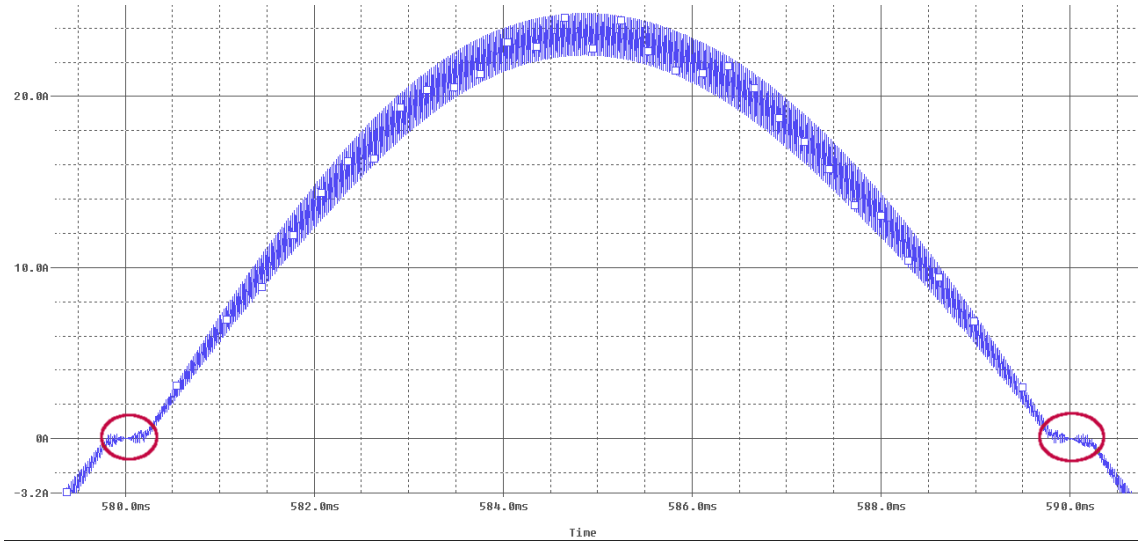

Figure 4.3: Frequency spectrums of different converters

The cause of this is the front voltage drop of the diodes and is impossible to totally remove when using diodes. During this project it was however found that the problem can be handled by changing the parameters for the current controlling PI-regulator. The current controller needs to be very fast in the start of the new period, thus a large proportional gain is needed. If the proportional gain was increased to much the current controller was however found to be unstable which gave rise to oscillation in the current.

4.2 Cost & Dimensional analysis

The amount of components was assumed large, the VAT is not included and the price found at distributors was divided by two. This was made to create the most likely scenario if any of the topologies were going to be used in a real car. The costs differed between the chargers, even though the same components were used in most of them, as all of them had different number of stages and number of components. In Table 4.2 the cost per unit for the components is shown and in Table 4.3 the number of components as well as the total cost is shown. Costs regarding production is neglected as it was assumed all chargers would fit in the same kind of enclosure and use the same kind of production techniques. This report focuses on pointing out the differences between the chargers and not the absolute cost.

Table 4.2: The price per unit for each of the components used.

Component	Price per unit
Diode	$0.93
MOSFET	$9.78
Capacitor	$8.55*
Inductor core	$14

*$9.62 for Fullbridge charger

Table 4.3: The number of components and the price for the converters.

Component	Diode	MOSFET	Capacitor	Inductors	Price
Conventional	6	2	4	2	$70.24
Bridgeless	3	3	4	3	$108.33
Fullbridge	0	4	4	2	$110.94*

*$5.34 added for MOSFET high side drivers.

In Table 4.4 the volume and weight are summarized, all values are calculated in 3.5.

Table 4.4: The total volume and weight from the major components.

Charger	Volume (dm^3)	Weight (kg)
Conventional	0.416	0.575
Bridgeless	0.562	0.738
Fullbridge	0.601	0.786

4.2.1 Total cost

To calculate which charger would be the best investment certain assumptions have to be made. The power consumption was estimated to $15\ \frac{kWh}{100km}$, these figures were taken from lectures about electricity in vehicles at Chalmers University of Technology. It was also assumed that a normal car is driven a total distance of $100\ km$ every day. Using these assumptions the total power consumption for all chargers were $15\ \frac{kWh}{day} = 15 \cdot 365 = 5475\ \frac{kWh}{year}$. As the chargers had different efficiency, the consumption was different for each charger, see Table 4.5. Also seen in Table 4.5 is the cost per year, where the cost per kWh was assumed to be $0.16.

Table 4.5: Total consumption for each charger.

	Efficiency	Consumption ($\frac{kWh}{year}$)	Cost per year
Conventional	96.06%	5699.56	$911.93
Bridgeless	97.80%	5598.16	$895.71
Fullbridge	97.91%	5591.87	$894.70

Notice that the efficiency for the bridgeless charger is somewhat lower. As the THD was high, a filter is most likely needed and it was assumed that the losses would increase with 0.37 percentage points. For calculation of the operation cost, net present value method was used with the discount rate as 5% and the life length of the chargers 15 years. For the bridgeless charger this gives a total operation cost as

$$NPV = \sum_{i=1}^{n} \frac{a_i}{(1+p)^i} = \sum_{i=1}^{15} \frac{895.71}{(1+0.05)^{15}} = 9297.2 \tag{4.1}$$

where i is the index for years, n is the life length of the charger, a_i is the cost every year and p is the discount rate. The operation costs for the other two chargers was calculated in the same was as in (4.1) and can be found in Table 4.6.

Table 4.6: Total cost for all the chargers for a life length of 15 years.

	NPV	Investment	Total cost
Conventional	$9465.5	$70.24	$9535.74
Bridgeless	$9297.2	$108.33	$9405.53
Fullbridge	$9286.7	$110.94	$9397.64

4.3 Thermal analysis

By simulation, the power losses on each component can be found and according to (2.8) in Section 2.4.1, and the temperature of each device can be calculated. In the reference design the maximum temperature allowed is $110°C$ and $95°C$ on the primary and secondary side respectively, thus that is the standard for selecting a heat sink in this project. Heat sink KS143.1-50E was found at ELFA and was finally chosen as the cooling component and the resulting temperatures is shown in Table 4.7.

Table 4.7: Temperature calculations for the components.

	Components	Losses (W)	Temperature ($°C$)	Explaination
Bridgeless	PM_PFC	9.98	45.65	MOSFET at PFC stage
	PD_PFC	11.86	68.89	Diode at PFC stage
	PM_buck	10.55	46.84	MOSFET at buck stage
	PD_buck	6.37	48.56	Diode at buck stage
Conventional	PD_Rec	21.43	104.31	Diode at Rectifier stage
	PM_boost	11.49	48.78	MOSFET at PFC stage
	PD_boost	23.98	113.71	Diode at PFC stage
	PM_buck	9.69	45.06	MOSFET at buck stage
	PD_buck	6.30	48.32	Diode at buck stage
Fullbridge	P1	16.94	60.06	MOSFET 1
	P2	16.69	59.55	MOSFET 2
	P3	16.61	59.39	MOSFET 3
	P4	16.52	59.20	MOSFET 4

As can be seen from the Table, in both the bridgeless and fullbridge charger, the maximum temperature is much lower than the requirement, therefore, heat sink and fan cooling system is sufficient in both cases. But in the conventional charger the temperature of rectifier bridge and diode at PFC stage is close to or higher than the requirement, so a larger heat sink or water cooling must be implemented to keep the temperature within the limits.

4.4 Risk analysis

Removing the galvanic isolation in the charger does have it's drawbacks as the safety is lower. All parts involved are encased and removing the isolation does not give rise to higher risk of personal injury. However, without the isolating transformer there is no upper power limit for the charger and a ground fault can cause very high currents to rush into the charger and destroy components. Of course all grid connections have fuses, as do the charger it self, but they are not always reliable and might not be fast enough to protect the charger and the battery in case of ground fault.

One way to at least partly solve this problem is to use a *Residual-Current Device* (RCD). A RCD measure the current both ways into the charger and if the current takes another path than the intended, it will cut the grid connection. A RCD breaks the current fast if the difference between phase and neutral is higher than $5 - 30\,mA$.

4.5 Implementation of synchronous rectification

Implementing synchronous rectification on the output stage can be one way to reduce the conducting losses. This is done by replacing the diode on the buck converter with a MOSFET. The conducting losses of a diode can be expressed as

$$P_{loss,diode} = V_{drop}I \tag{4.2}$$

where V_{drop} is the voltage drop over the series resistance. Likewise the losses for the MOSFET can be written as

$$P_{loss,MOSFET} = R_{ds}I^2 \tag{4.3}$$

where R_{ds} is the series resistance and I is the current through the component. Usually, the R_{ds} of a MOSFET is smaller than $100\,m\Omega$ and the forward voltage drop of the power diode is around $1.8\,V$. As can be seen from (4.2) and (4.3), the losses of a diode will be much bigger than MOSFET when the current is around $10\,A$.

Synchronous rectification requires a MOSFET driver which increases the complexity of the system and the cost of the product. But since the voltage drop of the diode is $3.6\,V$ and the R_{ds} of the MOSFET is only $28\,m\Omega$, it is worth testing the synchronous rectification.

Synchronous rectification was implemented in both the bridgeless and conventional converter. The only thing that changed was the diode in buck stage shown in figure 4.4.

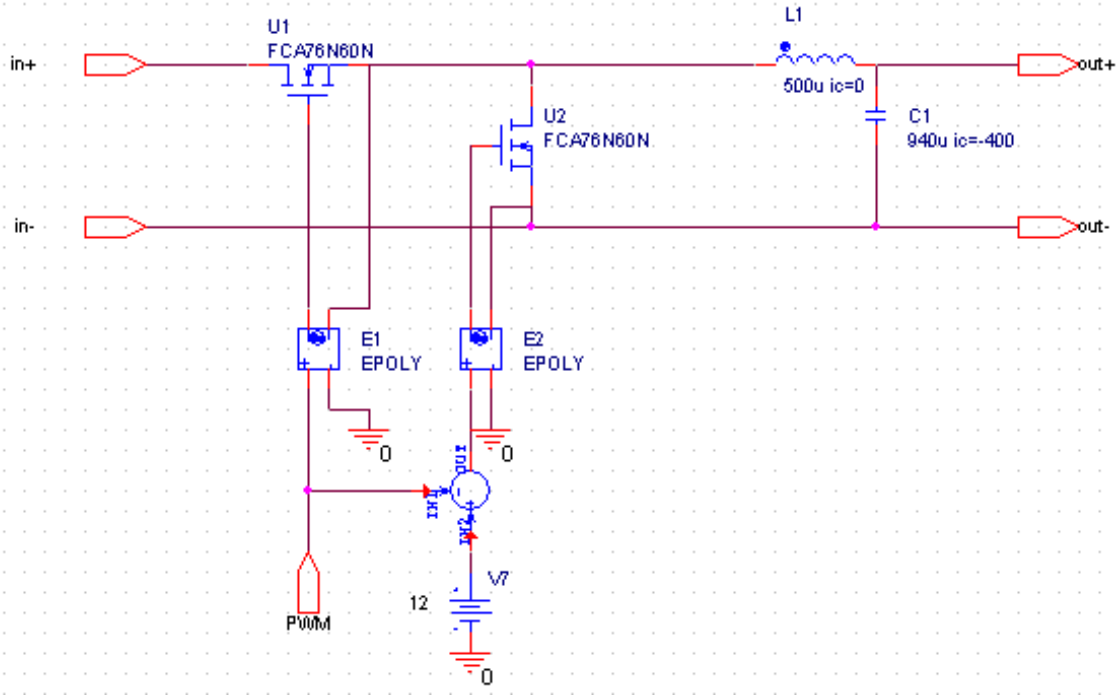

Figure 4.4: Circuit of buck converter with synchronous rectification

A MOSFET was put in place of the diode and the two MOSFET were controlled by opposite signal coming from PWM modulation block. The results of the synchronous rectification are shown in figure 4.8.

Table 4.8: Comparison of efficiency with and without synchronous rectification.

	With synchronous rectification	Without synchronous rectification
Conventional	95.84%	96.06%
Bridgeless	97.71%	98.17%

As shown, the efficiency of the converter with synchronous rectification is slightly lower than the original one in both cases, which is not as expected. When analyzing the switching pattern of one MOSFET the reason is visible, see figure 4.5.

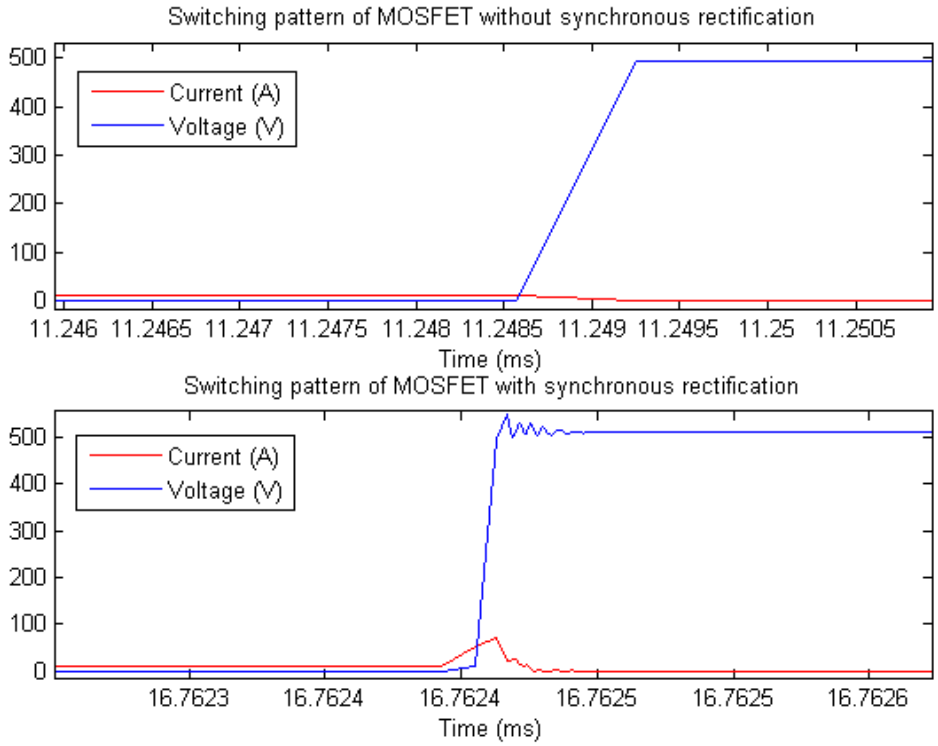

Figure 4.5: Switching pattern of the MOSFET

Since the switching losses during each switch period are quite different, only the average switching losses during each cycle can be estimated. This can be done by integrating all instantaneous power that is greater than $50\,W$ together to find the consumed switching energy. Therefore, the switching losses can be calculated by $P_{loss} = \frac{E_{loss}}{t_{total}}$. The switching losses for both case are presented in Table 4.9.

Table 4.9: Switching losses with and without synchronous rectification.

	Conventional		Bridgeless	
	With	Without	With	Without
MOSFET	14.22	7.89	15.79	8.79
Diode/MOSFET	11.60	2.13	12.36	2.02

Although the conducting losses can be reduced according to theoretical calculation, the switching losses of the MOSFET are increased dramatically. As a result, the total losses are increased. Therefore, it's not a good idea to implement synchronous rectification in this case.

Chapter 5

Conclusions

- Removing the galvanic isolation does increase efficiency
- The bridgeless charger is the most efficient, does however have drawbacks
- Safety is not necessarily lower
- Synchronous rectification is not a good solution in this case.
- With higher efficiency water cooling can be removed. Decreases the systems required power.

The final conclusion of this project with respect to efficiency, cost, dimensions and thermal analysis is that the bridgeless charger is the best choice. It is however in these simulations only the fullbridge converter who fulfill all the requirements. The possibility for improvement is however considered for the bridgeless as the only problem was the high amount of THD it injected into the utility. From this point in time it is hard to say if the bridgeless charger can perform better than the reference. To be able to draw that conclusion, a prototype have to be built. From the simulations it is however very clear that removing the galvanic isolation increase the efficiency. For all chargers the power factor was very high and in all cases higher than 99.9%

In case of personal safety there were no changes, but removing the galvanic isolation between the charger and the utility does increase the risk of damaging the charger a little bit. This risk is however possible to accept as the advantages are quite big.

As seen from the cost calculations there is no major difference between the bridgeless and the fullbridge. This is however very much dependent on the solution of the THD problem. Also worth noting is that the conventional charger is the worst charger in regards to costs even though the necessary improved cooling is not considered. Overall, removing the transformer decreases necessary volume, weight and price and lower losses makes the operation- and construction costs lower as there is no need for water cooling.

Table 5.1 is a summary of all the chargers attributes.

Table 5.1: Summary of the different chargers.

	Conventional	Bridgeless	Fullbridge
Efficiency	**Bad.** Efficiency was bad mostly because of the diode bridge. Efficiency decrease greatly with lower input voltage.	**Good.** High and almost constant efficiency for different power ratings and input voltage.	**Good.** More suitable for higher power ratings.
THD	**Acceptable.**	**Bad.** High amounts of THD in the input current. THD increased for 2.3kW case.	**Good.** Very low amount of THD in all cases. No crossover distortion.
Cost	**Good.** Was the cheapest charger.	**Acceptable.**	**Bad.** The most expensive charger.
Thermal	**Bad.** Need for water cooling for certain components.	**Good.** High efficiency results in low temperature.	**Good.** Even losses makes it easier to construct.
Other	Low amount of output voltage ripple but had three stages.	Low amount of output voltage ripple.	Only one stage, which is good. Did however have 100Hz ripple in output voltage.

5.1 Future work

Both the fullbridge and the bridgeless charger gave reason to investigate if it is possible to improve them more. Is it possible to decrease the cost of the fullbridge without impairing the performance to much? Can the THD of the bridgeless be decreased without influencing the cost? Is it possible to find another material with higher permeability for the inductor core, which can give higher input inductance without influencing the size of the component? This would give less ripple and/or lower losses as less turns might be needed. It might also be possible to increase the size of the output filter for the bridgeless and thus a second stage might not be necessary.

There might be a need for a soft starter for the chargers. In this project only steady state was considered but to decrease the strain on the grid and components as well as decreasing the amount of THD when the charger is started, the use of a soft starter might be necessary. To evaluate this, more focus have to be put into analyzing the start of the charger.

To further decrease the losses the use of *Zero Current Switching* or *Zero Voltage Switching* can be used. This means that the voltage over or current through the transistor during switching is zero and thus gives rise to a negligible amount of losses. This is done with a combination of diodes, inductors and capacitors. Using this method *Synchronous rectification* needs to be reevaluated as the switching losses was the reason for the lower performance.

Apart from further simulation and theoretical analysis the chargers can be constructed as a prototype to verify the results from the simulations. It is always important to build a prototype as the real circuit never works exactly as the simulation. Measurements have to be made to ensure it stays within the limits of the law and that the performance is as high as the simulations suggested.

References

[1] P. N. Ekemezie, "Design of a power factor correction ac-dc converter," in *AFRICON 2007*, 2007.

[2] Fca76n60n: N-channel mosfet. Fairchild Semiconductor. [Online]. Available: http://www.fairchildsemi.com/ds/FC/FCA76N60N.pdf

[3] N. Mohan, T. M. Undeland, and W. P. Robbins, *Power Electronics: Converters, Applications, And Design*, B. Zobrist, Ed. Wiley & Sons, INC., 2003.

[4] Stth1506dpi. ST Microelectronics. [Online]. Available: http://www.st.com/internet/analog/product/76408.jsp

[5] Specification for soft magnetic core: T60006-l2063-w985. Vacuumschmelze. [Online]. Available: http://www.vacuumschmelze.com/index.php?id=407

[6] Aluminum capacitors: Power long life 4-terminal snap-in. Vishay. [Online]. Available: http://www.vishay.com/docs/28392/096pll4t.pdf

[7] C. M. Wang, "A new single-phase zcs-pwm boost rectifier with high power factor and low conduction losses," *IEEE TRANSACTIONS ON INDUSTRIAL ELECTRONICS*, vol. 53, pp. 500–510, 2006.

[8] C. M. Wang, C. H. Su, C. H. Lin, M. Y. Liu, M. C. Jiang, and K. L. Fang, "A zvs-pwm voltage-doubler rectifier with high power factor," in *Industrial Technology*, 2008.

Appendix A

Control systems in PSpice

As most control systems are implemented with a DSP nowadays, the use of mathematical equations for the control system is favored as it creates a good overview and decrease complexity. With decreased complexity the required simulation time decreases and trouble shooting is easier. The alternative would be to create a control system with analog or digital ICs. This would create a lot of possible error sources and will result in a substantially longer simulation time. To be able to use mathematical equations in PSpice the library *ABM.OLB* needs to be imported, which is located in *INSTALLDIR\TOOLS\CAPTURE\LIBRARY\PSPICE*. With this library it is possible to create ideal PI-controllers and voltage- and current measurements. It is possible to add losses to the functions in order to create a more realistic control system, but this is only a constant power (W). In Table A.1 all the functions that was used in this project is shown.

Table A.1: Components used in the chargers.

Name	Function
ABS	Returns absolute value of input
CONST	A constant output
DIFF	Returns the difference between two inputs
GAIN	Multiplies the input with a certain gain
INTEG	Multiplies and integrate the input
LIMIT	Limits the input between a higher and lower limit
MULT	Returns the product of two inputs
SUM	Returns the sum of two inputs

If nothing else is shown, all inputs and outputs of the functions is considered to be voltage.

Appendix B

Components

Table B.1: Components used in the chargers.

Type	Manufacturer	Part number
Diode	STmicroeletronics	STTH1506DPI
MOSFET	Fairchild Semiconductor	FCA76N60N
Inductor core	Vacuumschmelze	T60006-L2063-W985

No specific component was found for the capacitor.

Appendix C

Losses in the converters

Conventional	Losses (W)	
	85 V	230 V
Diode in rectifier	22.94	21.43
MOSFET in PFC stage	32.86	11.49
Diode in PFC stage	9.32	23.98
MOSFET in buck	6.08	9.69
Diode in buck	1.93	6.30
Inductors at PFC stage	2.47	2.22
Inductors at buck stage	0.06	0.38
Capacitance at buck stage	0.11	0.13
Input power	1476.30	3785.54
Output power	1333.36	3636.49
Efficiency	90.32%	96.06%

(a) Losses for the conventional charger

Bridgeless	Losses (W)	
	85 V	230 V
MOSFET in PFC stage	9.99	9.98
Diode in PFC stage	5.70	11.86
MOSFET in buck	2.11	10.55
Diode in buck	0.19	6.37
2 inductors at PFC stage	2.28	2.4
Input power	1342	3714.41
Output power	1328.24	3635.92
Efficiency	98.97%	97.89%

(b) Losses for the bridgeless charger

Fullbridge	Losses (W)	
	85 V	230 V
MOSFET 1	16.31	16.94
MOSFET 2	16.70	16.69
MOSFET 3	16.43	16.61
MOSFET 4	14.87	16.52
2 inductors at PFC stage	2.52	2.38
Output capacitor	0.31	2.10
Input power	1408.44	3714.58
Output power	1333.35	3636.38
Efficiency	94.67%	97.90%

(c) Losses for the fullbridge charger

Table C.1: Losses for all the components in the chargers.